Journal of Hazardous Materials 217–218 (2012) 374–381

Contents lists available at SciVerse ScienceDirect

Journal of Hazardous Materials

journal homepage: www.elsevier.com/locate/jhazmat

# Adsorption of Cd(II) and Pb(II) onto a one step-synthesized polyampholyte: Kinetics and equilibrium studies

Guillermo J. Copello[a,b], Luis E. Diaz[a,b], Viviana Campo Dall' Orto[a,c,*]

[a] Department of Analytical Chemistry and Physical Chemistry, Faculty of Pharmacy and Biochemistry, University of Buenos Aires, Junín 956, 3rd floor, CABA 1113, Argentina
[b] IQUIMEFA (UBA-CONICET), Junín 956, CABA 1113, Argentina
[c] IQUIFIB (UBA-CONICET), Junín 956, CABA 1113, Argentina

ARTICLE INFO

*Article history:*
Received 27 November 2011
Received in revised form 29 February 2012
Accepted 15 March 2012
Available online 23 March 2012

*Keywords:*
Adsorption
Metal removal
Polyampholyte
Pb(II)
Cd(II)

ABSTRACT

A one step-synthesized polyampholyte, bearing carboxylate and 2-methylimidazole (2MI) groups, was tested as adsorbent for the removal of Pb(II) and Cd(II) from aqueous solutions. This material combines the benefits of synthetic polymers, such as high adsorption capacity and chemical stability, and the advantages of biosorbents in regard of costs and simplicity of the production.

The short time needed to achieve the adsorption equilibrium indicated a chemical-reaction controlled process. A network expansion was predicted as a result of repulsive interaction between the fixed positive charges.

Langmuir model presented the best fitting to isotherm equilibrium data, with a maximum adsorption capacity of 182 mg $g^{-1}$ for Cd(II) and 202 mg $g^{-1}$ for Pb(II). The metal removal was strongly dependent on pH, involving carboxylate and 2MI residues. An ion-exchange process for Pb(II) and Cd(II), combined with coordination for the later, were the most probable mechanism of interaction. The adsorption of 1.35 ppm Cd(II) was 72 ± 6% in well-water, and the adsorption of 0.50 ppm Pb(II) was 62 ± 5% in tap-water. The recovery figures for Cd(II) in 1% $HNO_3$ were optimal.



## 1. Introduction

The presence of heavy metals in wastewater, sediments and soils has its main source in anthropogenic activity and has become a major environmental issue due to their toxicity for living beings. Two of the most pollutant heavy metals are lead and cadmium, which are widely used in batteries manufacturing, alloys and pigments, among many others [1–3].

The traditional strategies for heavy metal removal from aqueous media are chemical precipitation, adsorption, membrane processes and dialysis. The application of these techniques is usually associated with high costs of production and regeneration [4]. For instance, chemical precipitation requires large amounts of reagents when treatment of large volumes of contaminated aqueous solutions is needed. In this regard the application of adsorption or ion exchange on solids is advantageous [5].

An efficient adsorbing material should consist of an insoluble porous matrix and some suitable active organic groups that interact with heavy metal ions [6,7]. The improvement of the ion exchange capacity and specificity is a challenge for researchers in the area of materials development.

A huge variety of innovative synthetic and hybrid adsorbents for heavy metals were recently reported [5–10]. Some of the novel polymers are zwitterions, containing both anionic and cationic functional groups in their structure endowing the material with wide spectrum sorption capacity [5,6].

In this work we tested a synthetic polyampholyte as sorbent for Pb(II) and Cd(II). The particular relevance of this material is that it combines the benefits of synthetic polymers, such as high adsorption capacity and chemical stability, and the advantages of biosorbents in regard of costs and simplicity of the obtaining procedure. It is synthesized in a one-step procedure and bears carboxylic and 2-methylimidazole residues which endows the material with adsorption capacity for metals, such as Cu(II) (67 mg $g^{-1}$) [11,12]. The polymer is chemically stable (resistant to acid and basic media, and to oxidizing agents such as hydrogen peroxide), and can be packed in the column of a flow system [13]. The adsorption kinetics and isotherms for Pb(II) and Cd(II) were modeled to obtain the parameters. Studies of selectivity were made and the analysis of real water samples spiked with Cd(II) was realized.

## 2. Experimental

### 2.1. Materials and reagents

2-Methylimidazole (2MI; 99 wt%), methacrylic acid (MAA; 99 wt%) and ethylene glycol diglycidyl ether (EGDE; 50 wt% in

* Corresponding author at: Department of Analytical Chemistry and Physical Chemistry, Faculty of Pharmacy and Biochemistry, University of Buenos Aires, Junín 956, 3rd floor, CABA 1113, Argentina. Tel.: +54 11 49648263; fax: +54 11 49648263.
*E-mail address:* vcdall@ffyb.uba.ar (V. Campo Dall' Orto).

0304-3894/$ – see front matter © 2012 Elsevier B.V. All rights reserved.
doi:10.1016/j.jhazmat.2012.03.045

ethylene glycol dimethylether) were purchased from Sigma–Aldrich. Benzoyl peroxide was purchased from Fluka. Acetonitrile from Baxter was of HPLC grade.

$Pb(NO_3)_2$ was purchased from Mallincrodt (USA). $Cd(NO_3)_2$ was acquired from Merck (Darmstadt, Germany). Nitric acid (70%) was purchased from J.T. Baker (Phillipsburg, NJ, USA). Water was filtered and deionized with a Milli-Q, Millipore system (Milford, MA, USA). All other reagents were of analytical grade. Standard stock solutions (1 g $L^{-1}$) of Cd(II) and Pb(II) were prepared and concentration verified against the appropriate dilution of Titrisol® Cadmium Standard 1000 mg $L^{-1}$ (Merck) and Chem Lab® Lead Standard 1000 mg $L^{-1}$ (Belgium). Tap-water samples from Buenos Aires city (Arg.) and ground-water samples from Temperley city (Buenos Aires province, Arg.) were collected and assayed without further treatment.

### 2.2. Polymer synthesis and conditioning

The polyampholyte was synthesized according to previous reports [11,12]. One milliliter of MAA, 2.0 mL of EGDE and 1.0 g of 2MI were mixed with 4.0 mL of acetonitrile. Then, 30 mg of benzoyl peroxide was added to the reaction. The solutions were placed in a tube glass and thermostated at 60 °C for 24 h. The material was placed at 20 °C, milled in particles, washed three times with distilled water and dried at 50 °C.

### 2.3. Adsorption experiments

They were carried out by a batch method (100 mL) at room temperature (25 °C) with constant stirring, using 0.025 g of the polyampholyte (Poly(EGDE-MAA-2MI)). Adsorption behavior of Cd(II) and Pb(II) was assayed in a range from 0.05 to 100 mg $L^{-1}$ and a pH range from pH 4 to 8. Adsorption kinetics and adsorption isotherms were determined by monitoring metal decay in the solution supernatant. After each experiment, solutions were ultracentrifuged and analyzed for the concentration of metals. For recovery and preconcentration assays Poly(EGDE-MAA-2MI) pellets were recovered and resuspended in 1% $HNO_3$. For selectivity and real water assays Cd(II) and/or Pb(II) were spiked in the water samples and incubated without conditioning.

For all tests, blank experiments were performed in order to verify that no chemical precipitation occurred. All experiments and measurements were conducted in triplicate under identical conditions.

### 2.4. Atomic absorption spectrophotometry

Metal determinations were done with a Buck Scientific VGP 210 Atomic Absorption Spectrophotometer (E. Norwalk, CT, USA) by the electrothermal atomization method using pyrolytic graphite tubes. Phosphate buffer (10 mM pH 7) and nickel nitrate 0.1% (w/v) were used as matrix modifiers for Cd(II) and Pb(II) determinations, respectively.

### 2.5. Polymer characterization

Elemental analysis was performed with a Carlo Erba EA 1108 device. Fourier transform infrared (FTIR) spectroscopy transmission spectra were acquired in the range of 4000–400 $cm^{-1}$ (Nicolet 360).

Potentiometric titrations of the solvated functional groups on the polyampholyte was carried out at 20 °C with a HANNA Instrument pH meter model HI 8424 supplied with a combined glass electrode [11,12].

The size and zeta potential ($\zeta$) of the particles were measured by Dynamic Light Scattering (DLS, Zetasizer Nano-Zs, Malvern Instruments, Worcestershire, UK) provided with a 4 mW He–Ne (633 nm) laser and a digital correlator ZEN3600, at 25 °C and constant ionic strength of $10^{-3}$ M KCl.

### 2.6. Determining isotherm parameters

The alternative isotherm parameter sets were determined by non-linear regression. The algorithm based on the Gauss–Newton method was used.

The error function employed to evaluate the fit was the second-order corrected Akaike information criterion ($AIC_C$):

$$AIC = N \ln\left(\frac{RSS}{N}\right) + 2P \quad (1)$$

$$AIC_C = AIC + \frac{2P(P+1)}{N-P-1} \quad (2)$$

where $P$ is the number of parameters in the model, $N$ the number of data points and RSS the residual squares sum [14].

$\Delta$AIC represents the difference in AIC values between two competing models. The associated Akaike weights for the better and worse models are:

$$W_{better} = \frac{1}{1+e^{-(1/2)\Delta AIC}} \quad (3)$$

$$W_{worse} = \frac{e^{-(1/2)\Delta AIC}}{1+e^{-(1/2)\Delta AIC}} \quad (4)$$

The Akaike weights provide information about the strengths of evidence supporting the two competing models. The ratio of the two Akaike weights, $W_{better}/W_{worse}$, is termed the evidence ratio and represents the relative likelihood favoring the better of two competing models. As reported by other authors, an evidence ratio greater than 20, would indicate extremely strong evidence favoring the better model [15].

## 3. Results and discussion

### 3.1. Synthesis and characterization of the polyampholyte

The material was synthesized via reaction of the selected monomers in the presence of benzoyl peroxide. Scheme 1 shows the most probable chemical structure for Poly(EGDE-MAA-2MI).

The mechanism of synthesis and the chemical structure of this material were studied by means of a variety of spectroscopic methods, and carefully described in previous reports [11,12,16]. Here we present the characterization of the polyampholyte production batch employed for the experiments of metal ions adsorption.

The elemental analysis of the Poly(EGDE-MAA-2MI) was C, 51.03; H, 8.19 and N, 5.98. This result indicated that the total amount of 2MI in the network was 2.13 mmol $g^{-1}$.

The isoelectric point (p$I$) for this material determined by the measurements of $\zeta$ was 6.77 (Supplementary data, Fig. A1). The apparent diameter of the particles was 64 ± 4 μm [13].

These particles have titrable carboxylate and 2MI residues (Supplementary data, Table A1), besides the hydroxyl groups (Scheme 1). The p$I$ calculated from the titrable functional groups (6.75) coincided with the value obtained from the $\zeta$ measurements [12].

If we compare the number of titrable 2MI and the total amount of 2MI determined by elemental analysis, only a 51.4% is accessible for $H^+$ exchange.

To analyze the electrostatic interaction between opposite charged ions, the empirical parameters of acidity can be deduced from

$$pH = pK^\circ + n \log\frac{\alpha_i}{1-\alpha_i} \quad (5)$$

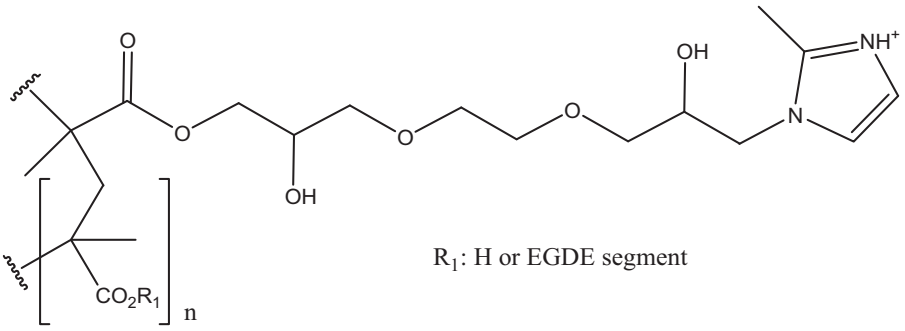


**Scheme 1.** Structure of Poly (EGDE-MAA-2MI).

$$pK = pK^{\circ} + (n-1)\log\frac{\alpha_i}{1-\alpha_i} \quad (6)$$

where $\alpha_i$ represents the acid dissociation degree for the carboxylic group or the $2MIH^+$ group, the p$K$ is the apparent acid dissociation constant for each acidic group and p$K^{\circ}$ is the p$K$ value at $\alpha_i = 0.5$. The p$K$ values are sensitive to this effect of opposite charges, and they can be obtained from pH and $\alpha_i$.

The values of $n$ from Eq. (6) exhibit the magnitude of the nearest neighbor interaction effect [11,12,17]. The empirical parameter $n$ was low for this polyampholyte when compared with polyelectrolytes and betaines, possibly due to the presence of neutral segments from the EGDE units acting as shields of the charged sites [18].

The p$K^{\circ}$ value of $CO_2H$ was higher than the p$K$ of the monomer, associated to the hydrophobicity and/or the degree of cross-linkage in the polymer (Supplementary data, Table A1) [19–21].

On the other hand, the p$K^{\circ}$ value of $2MIH^+$ was lower than the p$K$ of the monomer, probably associated to a distribution in cluster of these residues (Supplementary data, Table A1). The electrostatic repulsion between close neighbors would enhance the dissociation of $H^+$. The $n$ value was also slightly higher for these functional groups.

### 3.2. Effect of pH

The pH had a significant effect on the amount of immobilized ion (Supplementary data, Table A2), probably related to the degree of protonation of the binding sites on the polyampholyte surface. The p$I$ of this material was 6.77, so the surface net charge was close to zero around this point and became negative at higher pH values. From these results we selected pH 6.0 for Pb(II) and pH 7.0 for Cd(II) uptake from a 1.0 ppm solution, since the adsorption was close to 100%. Under these conditions, the species bound to the polyampholyte should be $Cd^{2+}$, $Cd(OH)^+$, $Pb^{2+}$ and $Pb(OH)^+$.

### 3.3. Cadmium and lead adsorption kinetics

In order to determine the rate-controlling step of the sorption process, the evolution of the adsorption capacity with time was studied. The experimental results are presented in Figs. 1 and 2.

The sorption mechanism could be controlled either by a chemical reaction or by diffusion processes, such as pore and film diffusion. The experiments were performed in a well-stirred batch system so the film diffusion should not be a major rate-controlling factor. Besides, these particles lack of mesopores, and the nanopores are not expected to be accessible for the cadmium or lead ions [22]. The relatively short contact time necessary to achieve equilibrium conditions is considered as an initial indication that the adsorption of the studied cations is a chemical-reaction controlled process (Figs. 1 and 2) [23–25]. Five kinetic models were used to fit the experimental adsorption data by non-linear regression: the

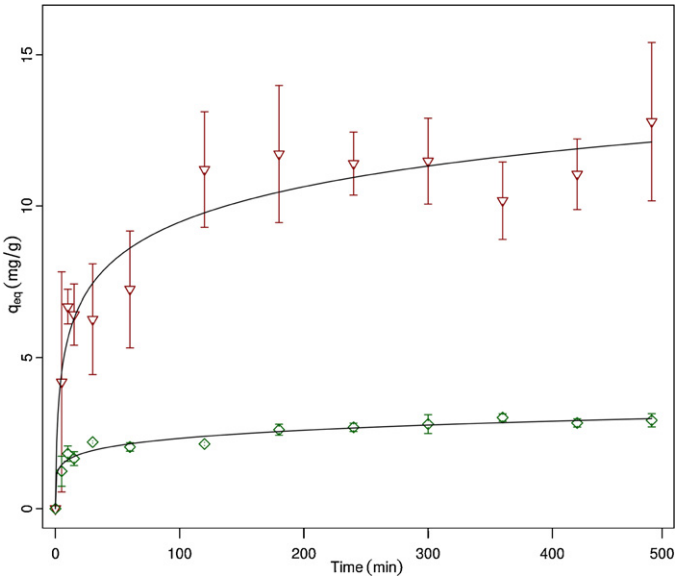


**Fig. 1.** Cd(II) adsorption onto the polyampholyte from a (▽) 5.98 mg $L^{-1}$ and from a (◇) 1.07 mg $L^{-1}$ solution as a function of contact time. Experimental data fitted to the Elovich model and to the modified Freundlich model, respectively.

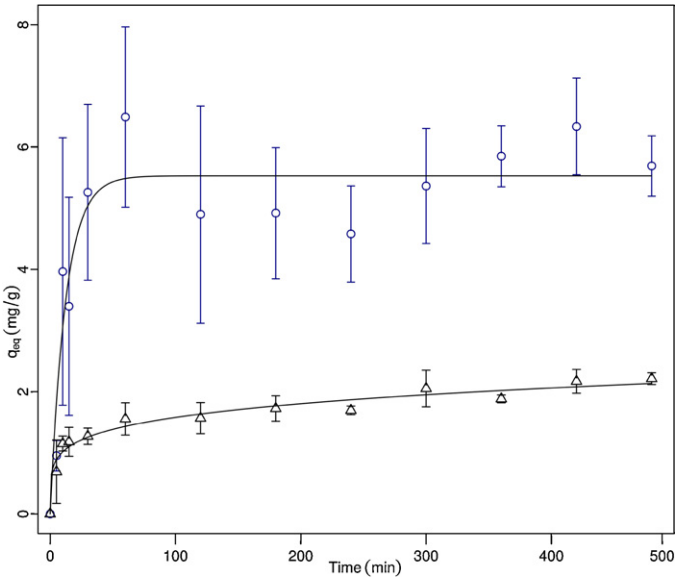


**Fig. 2.** Pb(II) adsorption onto the polyampholyte from a (○) 3.37 mg $L^{-1}$ and a (△) 0.81 mg $L^{-1}$ solution as a function of contact time. Experimental data fitted to the modified Freundlich model and to the pseudo-first order model with four parameters, respectively.

**Table 1**
Kinetic parameters for Cd(II) adsorption on the polyampholyte, regression coefficients and values of $AIC_C$ criterium for the best models.

| Metal ion | | Cd(II) | Cd(II) |
|---|---|---|---|
| $C_0$ (mg L$^{-1}$) | | 5.98 | 1.07 |
| Best model | | | |
| Elovich | | Modified Freundlich | |
| $\alpha$ (mg g$^{-1}$ min$^{-1}$) | 4.52 ± 2.80 | $m$ | 6.34 ± 0.55 |
| $\beta$ (g mg$^{-1}$) | 0.591 ± 0.077 | $k_F$ (L g$^{-1}$ min$^{-1}$) | 1.052 ± 0.075 |
| $R^2$ | 0.7222 | $R^2$ | 0.8780 |
| $AIC_C$ | 48.15 | $AIC_C$ | −98.07 |
| Evidence ratio | 1.00 | Evidence ratio | 1.00 |

**Table 2**
Kinetic parameters for Pb(II) adsorption on the polyampholyte, regression coefficients and values of $AIC_C$ criterium for the best models.

| Metal ion | | Pb(II) | Pb(II) |
|---|---|---|---|
| $C_0$ (mg L$^{-1}$) | | 3.37 | 0.81 |
| Best model | | | |
| Pseudo-first order with two parameters | | Modified Freundlich | |
| $q_e$ (mg g$^{-1}$) | 5.52 ± 0.25 | $m$ | 5.22 ± 0.56 |
| $k$ (min$^{-1}$) | 0.081 ± 0.019 | $k_F$ (L g$^{-1}$ min$^{-1}$) | 0.804 ± 0.089 |
| $R^2$ | 0.6006 | $R^2$ | 0.8258 |
| $AIC_C$ | 19.28 | $AIC_C$ | −98.71 |
| Evidence ratio | 1.00 | Evidence ratio | 1.00 |

pseudo-first order equation with two and with four parameters, the pseudo-second order equation, the Elovich equation, the intraparticle diffusion equation and the modified Freundlich equation (Supplementary data, Table A3). For cadmium adsorption at pH 7.0, the best fit of experimental adsorption data was obtained by means of the Elovich and the modified Freundlich models, according to the evidence ratio based on the Akaike criterion (Fig. 1, Table 1 and Supplementary data, Table A3).

The Elovich equation is based on a general second-order reaction mechanism for heterogeneous chemisorption processes, and is formulated as

$$\frac{dq_t}{dt} = \alpha e^{-\beta q_t} \tag{7}$$

where $q_t$ is the amount of adsorbed ion at the contact time $t$ [23,26].

After integration and applying the boundary conditions, for $q_t = 0$ at $t = 0$ and $q_t = q_t$ at $t = t$, the equation becomes [26]

$$q_t = \frac{1}{\beta} \ln(1 + (\alpha\beta t)) \tag{8}$$

Teng and Hsieh proposed that constant $\alpha$ is the initial adsorption rate and $\beta$ is related to the extent of surface coverage and the activation energy involved in chemisorption [27].

This equation assumes that the active sites of the sorbent are heterogeneous in nature and therefore exhibit different activation energies for chemisorption [26]. Another explanation for this form of kinetic law involves a variation of the energetics of chemisorption with the extent of surface coverage [27].

The constant $\alpha$ was observed to increase with the initial concentration of Cd(II), as expected (Table 1 and Supplementary data, Table A3). The constant $\beta$ decreased due to a smaller available sorption surface for the sorbates [26].

On the other hand, the modified Freundlich model was originally developed by Kuo and Lotse:

$$q_t = k_F C_0 (t^{1/m}) \tag{9}$$

where $k_F$ is the apparent adsorption rate constant, $C_0$ is the initial Cd(II) concentration and $m$ is the Kuo–Lotse constant [28]. This model can describe a surface diffusion-controlled process different from the intraparticle diffusion, involving the movement of the adsorbing ion along the walls of the less accessible spaces of the adsorbent. But for this polyampholyte, which lacks of mesopores, the cations will have an easy access to the exchange sites in the macropores, so the diffusion is not expected to rule the kinetics. Besides, the estimated $m$ parameter was significantly different from 2, confirming that the intraparticle diffusion in the nanopores was negligible, and it was independent from $C_0$ (Table 1 and Supplementary data, Table A3).

So in our case, the modified Freundlich model should be describing an adsorption rate-controlled process. Bache and Williams indicated that the energy of adsorption decreased exponentially with increasing surface saturation, due to an increase in the perturbation potential as a consequence of the interactions between the involved species [29]. The $k_F$ diminished when $C_0$ increased, in concordance with this theory (Table 1 and Supplementary data, Table A3).

For the particular case of the cadmium $C_0$ of 5.98 mg L$^{-1}$, the integrated forms of the pseudo-first order model with four parameters and of the pseudo-second order model had also statistical support (Supplementary data, Table A3).

The pseudo-first order model with four parameters involves two different types of binding sites, and in each case one ion sorbs to one active site:

$$q_t = q_{e1}(1 - e^{-k_1 t}) + q_{e2}(1 - e^{-k_2 t}) \tag{10}$$

where $q_e$ is the amount of cadmium sorbed at equilibrium as well as the equilibrium adsorption capacity of the sorbent, and $k$ is the rate constant. The subscripts 1 and 2 represent each type of binding site.

The pseudo-second order model is described by:

$$q_t = \frac{q_e^2 kt}{1 + (q_e kt)} \tag{11}$$

$$h = q_e^2 k \tag{12}$$

where $k$ is the rate constant of the pseudo-second order equation, and $h$ is the initial adsorption rate. The pseudo-second order kinetic model presupposes that each metal ion binds to the active sites on the surface in a 1:2 stoichiometric ratio [26,30].

The adsorption of Pb(II) was done at pH 6.0. Here, the equations that gave the most accurate fit to the experimental adsorption data varied with $C_0$ (Table 2 and Supplementary data, Table A3). When the adsorption capacity for lead was studied using a 0.81 mg L$^{-1}$ $C_0$, the more accurate fit to the experimental data was obtained with the modified Freundlich model, the Elovich model and the pseudo-first order model with four parameters (Table 2 and Supplementary data, Table A3). At this concentration level, the interaction between the bound species would affect the energy of adsorption with increasing saturation of the surface, as was observed for cadmium uptake.

The best fit of experimental adsorption data for 3.37 mg L$^{-1}$ $C_0$ was obtained by means of the integrated forms of the pseudo-first order model with two parameters and the pseudo-second order model (Table 2 and Supplementary data, Table A3). The equation of the pseudo-first order model is

$$q_t = q_e(1 - e^{-kt}) \tag{13}$$

The pseudo-first order kinetic model presupposes that each metal ion binds to one active site on the surface of the sorbent. The values of $h$ from the pseudo-second order model were affected by $C_0$, as expected. In the same way, other zwitterionic polymers

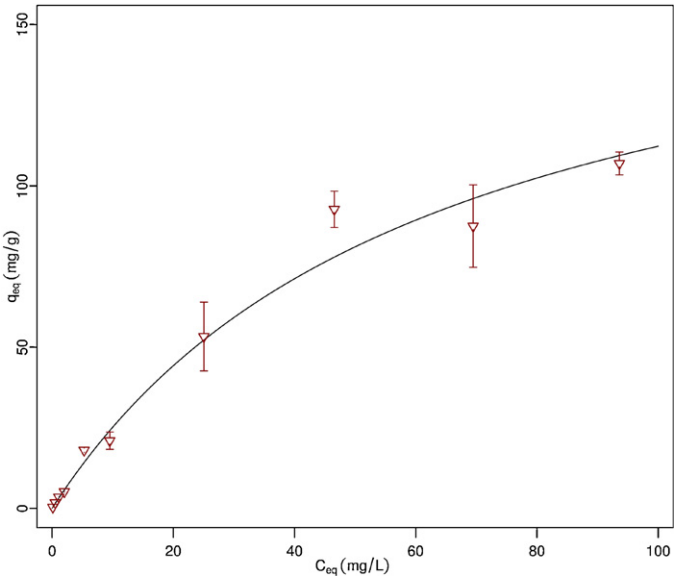


**Fig. 3.** Adsorption isotherm of Cd(II) onto the polyampholyte. Experimental data fitted to the Langmuir model.

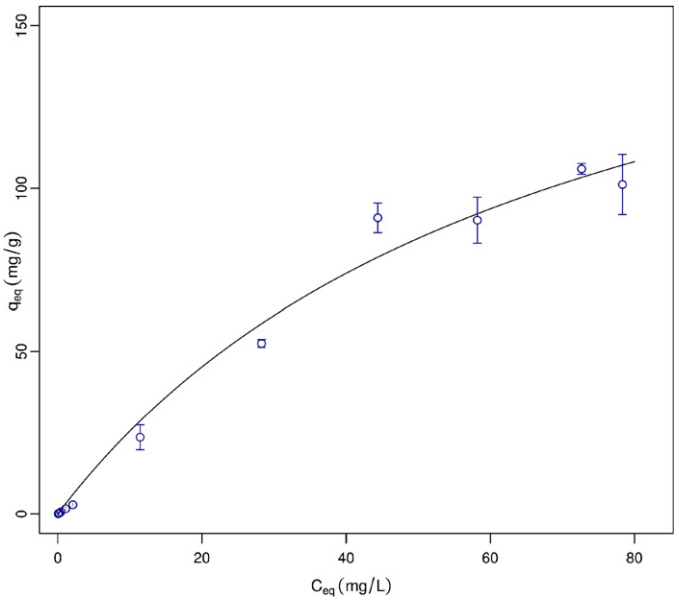


**Fig. 4.** Adsorption isotherm of Pb(II) onto the polyampholyte. Experimental data fitted to the Langmuir model.

reported in literature exhibited a kinetic profile for cation uptake described by the pseudo-second order equation [5].

The capacity of adsorption was observed to fluctuate at some point of each time profile (Figs. 1 and 2). This behavior was not described by any of the mathematical models tested with these results. It was attributed to repulsive interactions between the involved species, followed by conformational changes in the polyampholyte network that finally brought to the exposure of new binding sites for the metal ions.

In this sense, it must be remarked that the regression coefficients ($R$) for lead uptake at the $C_0$ of 3.37 mg $L^{-1}$ were significantly low, mainly affected by the evident fluctuation of sorption capacity at 120–300 min.

Then we can resume that the adsorption process ruled the kinetics in a first step, and the conformational change of the network determined the rate of adsorption in a second step. The kinetic laws that better fitted these results were those that described variations of the energetics of chemisorption with the extent of coverage due to interactions between the involved species.

### 3.4. Cadmium and lead adsorption equilibria

The mechanisms of cadmium uptake at pH 7.0 and of lead uptake at pH 6.0 were explored analyzing the results of the adsorption isotherms for the polyampholyte. Four isotherm models were used to fit the experimental adsorption data by non-linear regression: Langmuir, Dubinin–Radushkevich, Freundlich and Temkin.

For both cations, the best fit of experimental adsorption data was obtained by means of the Langmuir isotherm of one type of site, according with the evidence ratio based on the Akaike criterion (Tables 3 and 4, Figs. 3 and 4). The other tested models had no statistical support due to their significantly larger RSS. This model can be described as:

$$q_e = \frac{q_m C_e}{K_L + C_e} \tag{14}$$

where $C_e$ (mg $L^{-1}$) is the concentration of metal ion at equilibrium, $q_e$ is the adsorption capacity in equilibrium with the corresponding $C_e$, $q_m$ is the maximum adsorption capacity, and $K_L$ is the equilibrium constant of dissociation.

The change in free energy related to the ion uptake can be calculated from (Tables 3 and 4)

$$\Delta G^\circ = -RT \ln K_a \tag{15}$$

where $R$ (kJ $mol^{-1}$ $K^{-1}$) is the gas constant, $T$ is the thermodynamic temperature and $K_a$ ($M^{-1}$) is the equilibrium constant of association. The negative sign of the thermodynamic parameter indicated the spontaneous nature of the reaction.

The Langmuir equation assumes a homogeneous surface of the adsorbent, and there is no interaction between the adsorbed species on adjacent active sites [31]. The maximum adsorption capacity of this polyampholyte for Cd(II) (Table 3) and Pb(II) (Table 4) estimated from Langmuir equation were higher compared with other synthetic sorbents reported in literature [7,8,32], similar compared with some zwitterionic polymers and commercially available ion-exchange resins [5,6,33]and higher compared with other different biosorbents [34,35].

These results from the equilibrium did not correlate with the information coming from the kinetic models, which predicted a heterogeneous surface for adsorption. For this case, the Freundlich isotherm was expected to be the best model since it describes the reversible adsorption occurring on amorphous surfaces, not restricted to monolayer formation [36].

This apparent contradiction seems to find an explanation in the zwitterionic nature of the network. Exemplifying with the case of cadmium uptake, when the negative charge of $CO_2^-$ groups at pH 7.0 is screened by the incoming $Cd^{2+}$, there should be electrostatic repulsion between the $2MIH^+$ groups and the immobilized ions (coordination complexes and/or ion pairs; Scheme 2): $(CO_2Cd)^+$, $CO_2^-Cd^{2+}\cdots CO_2^-$, $(2MICd)^{2+}$ and less probable $((2MI)_2Cd)^{2+}$. As a consequence the network is expected to suffer a conformational change: an expansion known as “polyelectrolyte effect” [37]. This effect was also found in the binding of Cu(II) ions, and the consequent increment of mobility in the network could be determined by solid-state NMR [16].

The Langmuir model predicts that the adsorption energies of the active sites are equivalent on a homogeneous surface at the equilibrium. From the fit, we could conclude that these sites exposed as a consequence of the conformational changes had the same nature than the more accessible residues, at the equilibrium situation.

**Table 3**
Isotherm parameters for Cd(II) adsorption on the polyampholyte. Regression coefficients, values of $AIC_C$ criterium and evidence ratio for Langmuir, Dubinin–Radushkevich (D–R), Freundlich and Temkin models.

| Model | Parameters | | | $R^2$ | $AIC_C$ | Evidence ratio |
|---|---|---|---|---|---|---|
| Langmuir | $q_m$: 182 ± 19 mg g$^{-1}$ | $K_L$: 62 ± 13 mg L$^{-1}$ | $\Delta G^\circ$: −18.570 ± 0.087 kJ mol$^{-1}$ | 0.9711 | 115.58 | 1 |
| Dubinin–Radushkevich | $q_m$: 1.64 × 10$^3$ ± 0.38 × 10$^3$ mg g$^{-1}$ | $K_{DR}$: 5.08 × 10$^{-3}$ ± 0.40 × 10$^{-3}$ mol$^2$ kJ$^{-2}$ | $E$: 9.92 ± 0.35 kJ mol$^{-1}$ | 0.9627 | 122.96 | 40.18 |
| Freundlich | $K_F$: 6.0 ± 1.1 | $n$: 1.54 ± 0.11 | | 0.9567 | 127.29 | 349.03 |
| Temkin | $K_T$: 1.66 ± 0.53 L mg$^{-1}$ | $b$: 0.150 ± 0.016 kJ mol$^{-1}$ | | 0.7693 | 175.84 | 1 × 10$^{13}$ |

$q_e$ (mg g$^{-1}$) vs. $C_e$ (mg L$^{-1}$) except for D–R model in which $C_e$ is in g g$^{-1}$.

**Table 4**
Isotherm parameters for Pb(II) adsorption on the polyampholyte. Regression coefficients, values of $AIC_C$ criterium and evidence ratio for Langmuir, Dubinin–Radushkevich (D–R), Freundlich and Temkin models.

| Model | Parameters | | | $R^2$ | $AIC_C$ | Evidence ratio |
|---|---|---|---|---|---|---|
| Langmuir | $q_m$: 202 ± 23 mg g$^{-1}$ | $K_L$: 69 ± 15 mg L$^{-1}$ | $\Delta G^\circ$: −19.754 ± 0.093 kJ mol$^{-1}$ | 0.9825 | 118.10 | 1.00 |
| Dubinin–Radushkevich | $q_m$: 2.15 × 10$^3$ ± 0.38 × 10$^3$ mg g$^{-1}$ | $K_{DR}$: 5.43 × 10$^{-3}$ ± 0.40 × 10$^{-3}$ mol$^2$ kJ$^{-2}$ | $E$: 9.60 ± 0.36 kJ mol$^{-1}$ | 0.9774 | 126.30 | 60.25 |
| Freundlich | $K_F$: 5.3 ± 1.1 | $n$: 1.43 ± 0.11 | | 0.9731 | 131.83 | 956.41 |
| Temkin | $K_T$: 2.98 ± 0.98 L mg$^{-1}$ | $b$: 0.156 ± 0.014 kJ mol$^{-1}$ | | 0.8065 | 194.96 | 5 × 10$^{16}$ |

$q_e$ (mg g$^{-1}$) vs. $C_e$ (mg L$^{-1}$) except for D–R model in which $C_e$ is in g g$^{-1}$.

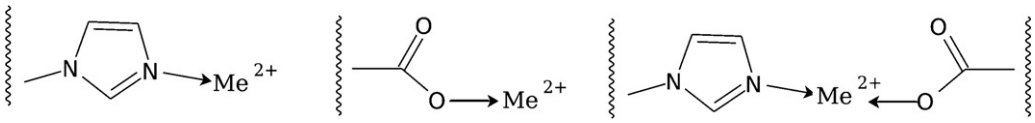


**Scheme 2.** Most probable structures of coordination complexes between each metal ion and the functional groups in the network.

### 3.5. Binding mechanism

In previous reports we found that this polyampholyte chemisorbs Cu(II) by means of coordination reactions which involve both $CO_2^-$ and 2MI ligands [38]. The mechanism of interaction between Pb(II), Cd(II) and adsorbents bearing $CO_2H$ and/or $-NH_2$ groups could be based on a coordination reaction, on a ion-exchange process, or a combination of both reactions [5–8,33,39–42]. The nature of the interaction between the polyampholyte and these cations appears to be chemical, involving the $CO_2^-$ and 2MI residues and affected by the pH.

A probable mechanism of interaction is the coordination of the free form of each metal with 2MI and/or $CO_2^-$ residues (energetically indistinguishable), and each cation would bind to only one site on the surface.

The ion-exchange is another possible mechanism that would involve the exchange of $Na^+$ associated to $CO_2^-$ and of $H^+$ associated to $CO_2H$. Here the cation would bind to the polymer by electrostatic attraction. The absence of changes in the FTIR spectrum of the polyampholyte at pH 7.0 with the uptake of Cd(II) (Supplementary data, Fig. A2) was consistent with an electrostatic interaction as a predominant process.

The mean free energy of sorption ($E$) derived from the Dubinin–Radushkevich equation (Tables 3 and 4) is useful for estimating the type of sorption reaction. An energy range from 8 to 16 kJ mol$^{-1}$ indicates ion-exchange process, and beyond 16 kJ mol$^{-1}$ a coordination reaction is expected. In our cases, and according with the $E$-magnitude, the most probable type of reaction would be ion-exchange.

The maximum adsorption capacity for Pb(II) estimated from Langmuir model was 0.98 mmol g$^{-1}$, which is close to the density of titrable $CO_2^-$ groups (0.86 mmol g$^{-1}$ at pH 6.0). The maximum adsorption capacity for Cd(II) was 1.6 mmol g$^{-1}$ and the density of total titrable residues was 1.98 mmol g$^{-1}$. This fact could be associated to the coordination of Cd(II) by 2MI residues and the release of $H^+$ [38], and/or to the exposition of more binding groups which were not available for titration but became accessible as a consequence of the network expansion.

### 3.6. Analysis of selectivity, real water samples and recovery

The selectivity of the polyampholyte toward Cd(II) and Pb(II) and its applicability on real water samples was evaluated by spiking ultrapure water, well-water and tap-water with different initial concentration of the metals. Table 5 shows the results of selectivity and real water sample assays.

The efficiency of ion uptake resulted strongly affected by the nature of the matrix. In first place, the composition of each sample matrix differs from the medium in which the isotherms were made (Supplementary data, Table A4).

It was observed that Cd(II) adsorption in ultrapure water did not differ significantly from the uptake in well-water (Supplementary data, Table A4). Nevertheless, the presence of Pb(II) greatly

**Table 5**
Adsorption of Cd(II) and Pb(II) in real water samples and in the presence of each metal.

| Metal | $C_0$ (mg L$^{-1}$) | Matrix | Adsorption (%) |
|---|---|---|---|
| Cd(II) | 1.55 ± 0.03 | 1 mg L$^{-1}$ Pb(II) | 10 ± 5 |
| | 1.35 ± 0.01 | Well-water | 72 ± 6 |
| | 1.10 ± 0.04 | Ultrapure | 80 ± 4 |
| | 0.600 ± 0.007 | Well-water | 79 ± 5 |
| | 0.52 ± 0.02 | Ultrapure | 83 ± 3 |
| Pb(II) | 1.00 ± 0.02 | 1 mg L$^{-1}$ Cd(II) | 65 ± 6 |
| | 1.1 ± 0.1 | Ultrapure | 35 ± 9 |
| | 0.50 ± 0.06 | Tap-water | 62 ± 5 |
| | 0.42 ± 0.02 | Ultrapure | 35 ± 5 |
| | 0.20 ± 0.02 | Tap-water | 38 ± 3 |
| | 0.21 ± 0.01 | Ultrapure | 30.1 ± 0.5 |

decreased Cd(II) adsorption. On the contrary, Pb(II) adsorption increased with the presence of Cd(II). This could be explained by the equilibrium constants of association calculated from the Langmuir model which would indicate that the sorbent will probably be more selective for Pb(II) than for Cd(II) or at least equilibrium will be favorable for Pb(II) adsorption (Pb(II): $K_a = 2.9\,L\,mmol^{-1}$; Cd(II): $K_a = 1.8\,L\,mmol^{-1}$). Besides, the best factor certainly affecting the adsorption capability of ions onto the same adsorbent is the covalent index proposed by Nieboer and Richardson [43], which is obtained by multiplying the square of electronegativity by the ionic radius. The index for $Pb^{2+}$ is twice higher than the index for $Cd^{2+}$, which should be understood as a more chelating affinity to the ligand relative to ionic interactions, and could explain the selectivity toward Pb(II) [7].

Pb(II) adsorption was also affected by the tap-water matrix. As it was observed for Cd(II) ions, the % of uptake was lower than 100%, attributed to a competition with other cations present in the matrix, such as $Na^+$, $Ca^{2+}$ and $Mg^{2+}$ for the binding sites in the polymer network (Supplementary data, Table A4). This matrix effect was more intense when a lower concentration of Pb(II) was tested, as expected.

When a matrix with higher saline content than ultrapure water was used, the presence of ions like $Ca^{2+}$ interacting with the polyampholyte would lead to electrostatic repulsion and finally an expansion in the polymeric network with the exposition of more binding sites [16]. On the other hand, water matrixes with low ionic strength would lead to a low expansion degree of the network, which would hide a certain amount of binding sites. This could explain the lower adsorption of Pb(II) when ultrapure water was used as matrix instead of tap-water. This effect might not have appreciable influence on Cd(II) adsorption, which has a lower ionic radio than Pb(II).

The recovery of the metals was evaluated by the adsorption of $0.063\,mg\,L^{-1}$ Cd(II) and its subsequent recovery in a volume 5 times smaller using 1% $HNO_3$ as eluent. Cd(II) was released from the polyampholyte within 2 h $HNO_3$ incubation. An amount equivalent to the 82.6% of the initial Cd(II) was recovered and the final concentration was four times more concentrated than the initial ($0.262\,mg\,L^{-1}$).

## 4. Conclusions

This stable polyampholyte holds great potential for the removal of Cd(II) and Pb(II) from water. The amount of immobilized ion was strongly influenced by the pH, probably related to the degree of protonation of the binding sites on the polyampholyte surface. The adsorption process controlled the kinetics of the ion uptake in a first step and the conformational change of the network determined the rate of adsorption in a second step. The kinetic model that better fitted these results were those that described variations of the energetics of chemisorption with the extent of coverage due to interactions between the involved species.

On the other hand, the Langmuir model fitted well the results from the binding equilibrium, predicting that the adsorption energies of the active sites were finally equivalent on the polyampholyte surface. The predominant type of reaction would be ion-exchange, according with FTIR results and the *E* derived from Dubinin–Radushkevich equation.

The polyampholyte adsorption performance demonstrated to be dependent to the sorbate and the water matrix. The uptake of Cd(II) from well-water was not different from the adsorption from ultrapure water, but was strongly affected by Pb(II) when the sample was spiked with this heavy metal. On the contrary, the uptake of Pb(II) was significantly dependent on soluble ions, including Cd(II).

These results suggest the potential application of a material which has the high adsorption capacity and chemical stability of synthetic adsorbents and is obtained in a simple procedure as natural biosorbents, with the possibility of being use in batch systems or packed columns.

## Acknowledgments

The authors specially thank the reviewers and editor for their helpful advice that contributed to improve this work. The authors thank the financial support from Universidad de Buenos Aires (UBACyT 08-10/B058; 10-12/20020090100237; 10-12/200200900085), CONICET (2010-2012/PIP 100076), ANPCyT (BID 1728/PICT 01778 and PICT-2010-1957).

## Appendix A. Supplementary data

Supplementary data associated with this article can be found, in the online version, at doi:10.1016/j.jhazmat.2012.03.045.

## References

[1] E. Berman, Toxic Metals and their Analysis, Heyden & Sons, London, 1980.
[2] M.P. Waalkes, Cadmium carcinogenesis in review, J. Inorg. Biochem. 79 (2000) 241–244.
[3] E.C. Foulkes, Biological Effects of Heavy Metals, CRC Press, Boca Raton, FL, 1990.
[4] B.L. Rivas, B. Quilodrán, E. Quiroz, Trace metal ion retention properties of crosslinked poly(4-vinylpyridine) and poly(acrylic acid), J. Appl. Polym. Sci. 92 (2004) 2908–2916.
[5] E. Ramírez, S.G. Burillo, C. Barrera-Díaz, G. Roa, B. Bilyeu, Use of pH-sensitive polymer hydrogels in lead removal from aqueous solution, J. Hazard. Mater. 192 (2011) 432–439.
[6] J. Liu, L. Song, G. Shao, Novel zwitterionic inorganic–organic hybrids: kinetic and equilibrium model studies on $Pb^{2+}$ removal from aqueous solution, J. Chem. Eng. Data 56 (2011) 2119–2127.
[7] A. Shahbazi, H. Younesi, A. Badiei, Functionalized SBA-15 mesoporous silica by melamine-based dendrimer amines for adsorptive characteristics of Pb(II), Cu(II) and Cd(II) heavy metal ions in batch and fixed bed column, Chem. Eng. J. 168 (2011) 505–518.
[8] R.K. Misra, S.K. Jain, P.K. Khatri, Iminodiacetic acid functionalized cation exchange resin for adsorptive removal of Cr(VI), Cd(II), Ni(II) and Pb(II) from their aqueous solutions, J. Hazard. Mater. 185 (2011) 1508–1512.
[9] M.M. Motsa, B.B. Mamba, J.M. Thwala, T.A.M. Msagati, Preparation, characterization, and application of polypropylene–clinoptilolite composites for the selective adsorption of lead from aqueous media, J. Colloid Interface Sci. 359 (2011) 210–219.
[10] G.J. Copello, F. Varela, R. Martinez Vivot, L.E. Diaz, Immobilized chitosan as biosorbent for the removal of Cd(II), Cr(III) and Cr(VI) from aqueous solutions, Bioresour. Technol. 99 (2008) 6538–6544.
[11] J.M. Lázaro Martínez, M.F. Leal Denis, V. Campo Dall'Orto, G.Y. Buldain, Synthesis, FTIR, solid-state NMR and SEM studies of novel polyampholytes or polyelectrolytes obtained from EGDE, MAA and imidazoles, Eur. Polym. J. 44 (2008) 392–407.
[12] M.F. Leal Denis, R.R. Carballo, A.J. Spiaggi, P.C. Dabas, V. Campo Dall' Orto, J.M.L. Martínez, et al., Synthesis and sorption properties of a polyampholyte, React. Funct. Polym. 68 (2008) 169–181.
[13] L.R. Denaday, M.V. Miranda, R.M. Torres Sánchez, J.M. Lázaro Martínez, L.V. Lombardo Lupano, V. Campo Dall' Orto, Development and characterization of a polyampholyte-based reactor immobilizing soybean seed coat peroxidase for analytical applications in a flow system, Biochem. Eng. J. 58-59 (2011) 57–68.
[14] M. Hadi, M.R. Samarghandi, G. McKay, Equilibrium two-parameter isotherms of acid dyes sorption by activated carbons: study of residual errors, Chem. Eng. J. 160 (2010) 408–416.
[15] K. Burnham, D. Anderson, K. Huyvaert, AIC model selection and multimodel inference in behavioral ecology: some background, observations, and comparisons, Behav. Ecol. Sociobiol. 65 (2011) 23–35.
[16] J.M. Lázaro Martínez, A.K. Chattah, G.A. Monti, M.F. Leal Denis, G.Y. Buldain, V. Campo Dall' Orto, New copper(II) complexes of polyampholyte and polyelectrolyte polymers: solid-state NMR, FTIR, XRPD and thermal analyses, Polymer 49 (2008) 5482–5489.
[17] M. Casolaro, S. Bottari, A. Cappelli, R. Mendichi, Y. Ito, Vinyl polymers based on l-histidine residues. Part 1. The thermodynamics of poly(ampholyte)s in the free and in the cross-linked gel form, Biomacromolecules 5 (2004) 1325–1332.
[18] S. Racovita, S. Vasiliu, V. Neagu, Solution properties of three polyzwitterions based on poly(N-vinylimidazole), Iran. Polym. J. 19 (2010) 333–341.
[19] O.E. Philippova, D. Hourdet, R. Audebert, A.R. Khokhlov, pH-responsive gels of hydrophobically modified poly(acrylic acid), Macromolecules 30 (1997) 8278–8285.

[20] V. Soldatov, Potentiometric titration of ion exchangers, React. Funct. Polym. 38 (1998) 73–112.
[21] I. Michaeli, A. Katchalsky, Potentiometric titration of polyelectrolyte gels, J. Polym. Sci. 23 (1957) 683–696.
[22] J.M. Lázaro Martínez, M.F. Leal Denis, L.R. Denaday, V. Campo Dall' Orto, Development and characterization of a new polyampholyte–surfactant complex applied to the solid phase extraction of bisphenol-A, Talanta 80 (2009) 789–796.
[23] A.B. Pérez-Marín, V.M. Zapata, J.F. Ortuño, M. Aguilar, J. Sáez, M. Lloréns, Removal of cadmium from aqueous solutions by adsorption onto orange waste, J. Hazard. Mater. 139 (2007) 122–131.
[24] Y.S. Ho, G. McKay, The kinetics of sorption of divalent metal ions onto sphagnum moss peat, Water Res. 34 (2000) 735–742.
[25] M.X. Loukidou, A.I. Zouboulis, T.D. Karapantsios, K.A. Matis, Equilibrium and kinetic modeling of chromium(VI) biosorption by Aeromonas caviae, Colloids Surf. A 242 (2004) 93–104.
[26] C. Cheung, J. Porter, G. Mckay, Sorption kinetic analysis for the removal of cadmium ions from effluents using bone char, Water Res. 35 (2001) 605–612.
[27] H. Teng, C.-T. Hsieh, Activation energy for oxygen chemisorption on carbon at low temperatures, Ind. Eng. Chem. Res. 38 (1998) 292–297.
[28] S. Kuo, E.G. Lotse, Kinetics of phosphate adsorption and desorption by hematite and gibbsitel, Soil Sci. 116 (1973).
[29] B.W. Bache, E.G. Williams, A phosphate sorption index for soils, J. Soil Sci. 22 (1971) 289–301.
[30] Y. Ho, G. McKay, Pseudo-second order model for sorption processes, Process Biochem. 34 (1999) 451–465.
[31] I. Langmuir, The adsorption of gases on plane surfaces of glass, mica and platinum, J. Am. Chem. Soc. 40 (1918) 1361–1403.
[32] B. Bagheri, M. Abdouss, M.M. Aslzadeh, A.M. Shoushtari, Efficient removal of $Cr^{3+}$, $Pb^{2+}$ and $Hg^{2+}$ ions from industrial effluents by hydrolyzed/thioamidated polyacrylonitrile fibres, Iran. Polym. J. 19 (2010) 911–925.
[33] Z. Reddad, C. Gerente, Y. Andres, P. Le Cloirec, Adsorption of several metal ions onto a low-cost biosorbent: kinetic and equilibrium studies, Environ. Sci. Technol. 36 (2002) 2067–2073.
[34] J. Febrianto, A.N. Kosasih, J. Sunarso, Y.-H. Ju, N. Indraswati, S. Ismadji, Equilibrium and kinetic studies in adsorption of heavy metals using biosorbent: a summary of recent studies, J. Hazard. Mater. 162 (2009) 616–645.
[35] R. Pan, L. Cao, R. Zhang, Combined effects of Cu, Cd, Pb, and Zn on the growth and uptake of consortium of Cu-resistant *Penicillium* sp. A1 and Cd-resistant *Fusarium* sp. A19, J. Hazard. Mater. 171 (2009) 761–766.
[36] H. Freundlich, Ueber die adsorption in loesungen, Z. Phys. Chem. 57 (1907) 385–470.
[37] A.B. Lowe, C.L. McCormick, Synthesis and solution properties of zwitterionic polymers, Chem. Rev. 102 (2002) 4177–4190.
[38] J.M. Lázaro Martínez, E. Rodríguez-Castellón, R.M.T. Sánchez, L.R. Denaday, G.Y. Buldain, V. Campo Dall' Orto, XPS studies on the Cu(I,II)–polyampholyte heterogeneous catalyst: An insight into its structure and mechanism, J. Mol. Catal. A: Chem. 339 (2011) 43–51.
[39] K.F. Lam, K.L. Yeung, G. McKay, Efficient approach for $Cd^{2+}$ and $Ni^{2+}$ removal and recovery using mesoporous adsorbent with tunable selectivity, Environ. Sci. Technol. 41 (2007) 3329–3334.
[40] P. Miretzky, A. Saralegui, A. Fernández Cirelli, Simultaneous heavy metal removal mechanism by dead macrophytes, Chemosphere 62 (2006) 247–254.
[41] A. Khan, S. Badshah, C. Airoldi, Biosorption of some toxic metal ions by chitosan modified with glycidylmethacrylate and diethylenetriamine, Chem. Eng. J. 171 (2011) 159–166.
[42] G.J. Copello, A.M. Mebert, M. Raineri, M.P. Pesenti, L.E. Diaz, Removal of dyes from water using chitosan hydrogel/$SiO_2$ and chitin hydrogel/$SiO_2$ hybrid materials obtained by the sol–gel method, J. Hazard. Mater. 186 (2011) 932–939.
[43] E. Nieboer, D.H.S. Richardson, The replacement of the nondescript term 'heavy metals' by a biologically and chemically significant classification of metal ions, Environ. Pollut. B 1 (1980) 3–26.